ACADEMY OF ROMANIAN SCIENTISTS

NEW APPROACH IN MACHINING:
TURNING AND DRILLING APPLICATION

Edited by: Alain GERARD and Miron ZAPCIU

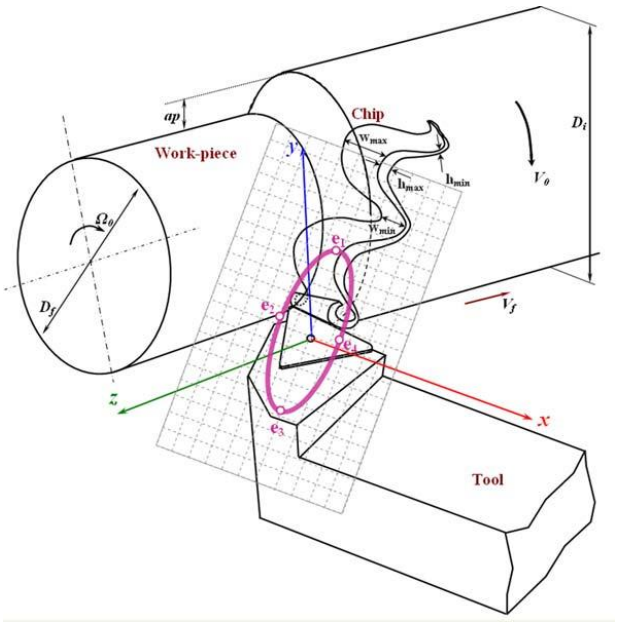

Academy of Romanian Scientists Publishing House
2010

Editors:

Alain Gerard, Université Bordeaux 1 (Sciences et Technologies) et CNRS Laboratoire de Mécanique Physique UMR 5496, 351 cours de la Libération, 33405 Talence, France, Prof., Dr., e-mail: alain.gerard@u-bordeaux1.fr.

Miron Zapciu, University „Politehnica" of Bucharest, 313 Splaiul Independenței, MSP, 60042 Bucharest, Romania. Prof., Dr., Eng., e-mail: zapcium@yahoo.com.

Academy of Romanian Scientists Publishing House

Adress: *Splaiul Independenței, no. 54, sector 5, cod 050094, Bucharest, Romania*

Descrierea CIP a Bibliotecii Naţionale a României

New Approach in Machining: Turning and Drilling Application

prof. Alain Gerard, prof. Prof. Miron Zapciu / Bucureşti:

Editura Academiei Oamenilor de Ştiinţă din România, 2010

Bibliogr.

Index

ISBN 978-606-92161-8-7

I. ZAPCIU, Miron

621.9

Chief of Department: Liviu Mihai SIMA, Academy of Romanian Scientists Publishing House, Bucharest, eng., Ph.D. (A.B.D.), University „Politehnica" of Bucharest, Romania.

Redactor: Andrei D. PETRESCU, Academy of Romanian Scientists Publishing House, prof. National College "Gheorghe Lazăr", Ph.D. (A.B.D.), University „Politehnica" of Bucharest, Romania.

Documentalist: Ioan BALINT, Academy of Romanian Scientists Publishing House, eng.

CONTENTS

FOREWORD

Matter removal remains nowadays a major process in the manufacture of objects or structures. Whatever the process of machining used (milling, turning, drilling, etc), the removal of matter is accompanied by translation motion (linear motion) and rotation (circular motion).

Through the principle of the virtual powers, these rotation and translation motions are, mathematically speaking, the dual elements of the forces and the moments. The taking into account of this duality led us not to restrict us with the only concept of force and to hold account in a systematic way of the moments in the manufacture process by matter removal. Thus, it was shown that the taking into account of the forces and the moments, leads to outputs of the machine tools completely comparable with those of the electrical motors traditional (Cahuc et al. 2001; Dargnat et al. 2008).

Considering these results, it is clear that a complete modelling of the matter removal must take into account at the same time the concept of force and that of moment necessarily concerned in these manufacturing processes (Cahuc, 2005). In other words, a real three-dimensional modelling of the materials cut must necessarily call upon the concept of force and moment, or better of torsor, as with the consequences that involves. It is precisely the objective of this book which is based on our work of the last decade with in particular two examples of application which are turning (Part 1) and drilling (Part 2).

Obviously, metrology plays an important role to achieve the goal of a three-dimensional cut modelling. Thus, a large space is reserved to cutting forces. These are acquired by a dynamometer with six components which allow us simultaneously to reach the three components of the forces and the three components of the moments. The torsor concept plays a central role for the continuation of the developments. The translations and rotations are measured in the same way. In the case of turning, in particular, it is established an excellent correlation between efforts (forces and moments) and displacements (translations and rotations).

Thus, this book is structured in two parts. These are independent and classically preceded by an introduction (cf chapter 2). The vector analysis and torsor concept are recalled to the chapter 3. Also, the reader which is familiar to this concept can move on directly to chapter 4. This one relates to the static characterization of a lathe. The concept of torsor appears with small displacements of translation and rotation which leads to its definition, rotation centre and stiffness centre.

The dynamic characterization aspects of the machine tools are the object of chapter 5. Thus, it is given a certain number of recommendations to have the best possible management of the cutting process.

The complete measurement of the tool displacements torsor is the object of the 6th chapter. It is shown that the tool has "on average" an elliptic way located in a tilted plan compared to the machine axes. It is established a correlation between the stiffness centre and the ellipse attached of the tool tip displacements. This ellipse is more or less flattened, according to the rate of vibrations related to the machining process. Thus, the small axis of the ellipse of displacements is characteristic to the rate of vibrations and it is a potential parameter of the surface quality of the machined part. Within the chapter 7 the measurement of the forces and the moments of cut is shown. The moment concept leads to many new results. The link with the displacements torsor is carried out. The meticulous study of the forces torsor is carried out. For the set of tests carried out, the examination of the moments of the forces to the central axis shows a link between the evolution of certain components of the moments and the direction of the chips ejection, for example.

The second part was essentially divided into three stages differentiated and complementary to modelling of the physical phenomena induced by the process of drilling. The first stage (chapter 11) lies in describing the real geometrical parameters according to the parameters of grinding of the tool. While being based on the modelling of the geometry, the experimental cutting model wants to identify the mechanical actions of cutting along the edge (chapter 12). Lastly (chapter 13), the phenomenological aspect of the process, associates the parameters of cut the final quality of the bored holes.

Professor Alain GERARD

Université de Bordeaux (Bordeaux 1) and CNRS UMR 5469 - France

Professor Miron ZAPCIU

University „Politehnica” of Bucarest, Romania

PACS 05.45 -a; 46-32.x, 96.50.Fm. **Keywords**: Mechanical Engineering.

Keywords: Experimental mode; Displacement plan; Self-excited vibrations; Dynamic characterization; Machining system; Natural frequencies analysis; Torsor measurement; Torsor central axis; Turning

AMS Subject Classification: 53D, 37C, 65P.Nomenclature

1 NOMENCLATURE

A	Central axis point
$[A]_o$	Actions torsor exerted on the tool tip in O point
a	Distance between displacement transducer
ap	Depth of cut (mm)
a_u (b_u)	Large (small) axis of ellipse attached with the cutting tool tip displacements (m)
a_f (b_f)	Large (small) axis of ellipse attached with theforces charge points (m)
BT	Block Tool
BW	Block Workpiece
[C]	Damping matrix
$[C_o]$	Compliance matrix
C_i	Displacement transducer (i =1 to 6)
$\mathbf{CR}_{BT}$	Block Tool **BT** stiffness cntre
D_1	Holding fixture diameter (mm)
D_2	Workpiece diameter (mm)
$\{D_{ij}\}$	Straight line corresponding of the displacement direction of the point P_{ij} (i = x, y, z) and (j=1, 2, 3)
{D}	Small displacements torsor
d_{ij}	Points displacements vectors P_{ij} (i = x, y, z) and (j=1, 2, 3)
d_x	Distance between the line D_{ij}
E	Young modulus (N/mm²)
e_x , f_x	Scale factors
F_i	Force vectors applied to obtain **BT** stiffness centre (i = x, y, z)
I	Inertial moment
f	Feed rate (mm/rev)
$f_{sampling}$	Sampling frequency (Hz)

f_{max}	Highest frequency component in the measured signal (Hz)
[K]	Stiffness matrix (N/m)
$[K_C]$	Stiffness matrix of rotation (N.m/rad)
$[K_F]$	Stiffness matrix of displacement (N/m)
N	Number of revolutions (rpm)
$\mathbf{n_f}$	Vector attached to the components system stiffness
$\mathbf{n_u}$	Normal direction of the plane P_u
$\mathbf{n_{ui}}$	Unitary vector, support of the ellipse axis i (i= a,b) situated in the plane P_u
P_u	Plane attached with the cutting tool edge displacements
r_ε	Cutting edge radius (mm)
R	Cutting tool edge radius (mm)
R_t	Total roughness (μm)
$[K_{F,BT}]$	Stiffness matrix of **BT** displacement (N/m)
$[K_{F,BW}]$	Stiffness matrix of **BW** displacement (N/m)
$[K_{F,WAM}]$	Stiffness matrix of machining system displacement (N/m)
$[K_{errors}(\%)]$	Errors matrix for the matrix [K]
$[K_{CF}]$	Stiffness matrix of rotation / displacement (Nm/m)
$[K_{FC}]$	Stiffness matrix of displacement /rotation (N/rad)
L_1	Holding fixture length (mm)
L_2	Length workpiece (mm)
M_i	Point intersection between straight lines (Dij) (i = x, y, z) and (j=1,2,3)
m	Displacement measured at the charge point
[M]	Mass matrix
n_i	Plan normal P_i
O	Tool tip point
O_c	Cub cntre
P	Force (N)

P_i	Plan including the point M_i
P_{BT}	Displacement plan considering tool point
d_i	Directory line of moments projection at the central axis (i = 1, 2)
e_i	Ellipse point belong attached of forces application points (i = 1-5)
F_v (F_n)	Variable (nominal) cutting force (N)
F_x	Effort along cross direction (N)
F_y	Effort along cutting axis (N)
F_z	Effort along feed rate axis (N)
h_{max}	Maximum chip thickness (mm)
h_{min}	Minimum chip thickness (mm)
l_o	Chip undulation length (mm)
$\mathbf{M_A}$	Cutting forces minimum moment in A that act on the tool (dN.m)
Mo	Cutting forces moment in the O point that act on the tool (dN.m)
n_{fa} (n_{fb})	Normal direction projection to the P_f on the a_f (b_f)
O’	Dynamometer centre transducer
P_f	Plane attached at the forces application points
P_{ij}	Charge points (i = x, y, z) and (j=1, 2, 3)
T	Period (s)
{T}	Mechanical actions torsor
u	Tool edge point displacement (m)
α	Clearance angle (degree)
$\alpha_{\kappa(xy)}$	Angle of the main stiffness direction in the plane (x,y) (degree)
$\alpha_{\kappa(yz)}$	Angle of the main stiffness direction in the plane (y,z) (degree)
Δt	Temporal dephasing between two signals (s)
φ_u	Dephasing between the displacements components attached at the tool edge point (degree)
γ	Cutting angle (degree)
λ_s	Inclination angle of edge (degree)
κ_r	Direct angle of the cutting edge (degree)

$\theta_{e(xy)}$	Main displacements direction angle of the tool edge point in the plane (x,y)
[V]	Matrix eigenvector [$K_{F,BT}$]
v_1	Matrix eigenvalue [$K_{F,BT}$]
R	Cutting forces vector sum which act on the tool (N)
V	Cutting speed (m/min)
w_{max}	Maximum chip width (mm)
w_{min}	Minimum chip width (mm)
WTM	Workpiece-Tool-Machine
x (**z**)	Cross (feed) direction
y	Cutting axis
Φ	Primary share angle (degree)
φ_{fui}	Phase difference between the tool tip displacements components i=x, y, z (degree)
ξ_c	Chip hardening coefficient
δ	Displacement (mm)
ε_i	Displacement along i (i=1,2,3)
θ	Measured angle at the force point
θ_i	Angular deviation of "Co-planarity" between lines Dij (i = x, y, z; and j=1, 2, 3)
μ_i	Minimal distance between straight lines Dij (i = x, y, z; and j=1, 2, 3)
ω_d	Damped natural frequency
ξ_i	Percentage of damping
ρ_i	Rotation along i (i=x, y, z)

2 INTRODUCTION

ALAIN GERARD, MIRON ZAPCIU

Metal cutting is one of the most important manufacturing processes. Among the various manufacturing processes to remove excess material, milling, drilling, grinding, turning it occupies an important place.

This process is usually used in many circumstances as the outline of the parts for example, but also as soon as requirements of dimensional tolerance, precision or the surfaces quality of the produced part appear.

During the cutting process of different materials, a whole of physic-chemical and dynamic phenomena are involved. Elasto-plastic strains, friction and thermal phenomena are generated in the contact zone between workpiece, tool and chip. These phenomena are influenced by: physical properties of the material to be machined, tool geometry, cutting and lubrication conditions, and the machining system dynamic parameters (stiffness, damping).

The machine tool vibrations are generated by the interaction between the elastic machining system and the cutting process. The elastic system is composed of: the different parts of the machine tool in movement, the workpiece and the tool. Actions of the machining process are usually forces and moments.

These actions also generate relative displacements of elements composing the elastic system. They occur, for example, between the tool and workpiece, the tool device and bed, etc. These displacements modify the cutting conditions and in the same way the forces. Thus, the knowledge of the machining system elastic behaviour is essential to understand the cutting process (Cano et al 2008).

Certain scientists developed a finite element beam model of spinning stepped-shaft workpiece to perform stability analysis using Nyquist criterion (Wang et al 2002) or the traditional stability lobe diagram (Ganguli et al 2007; Seguy et al 2008; Thevenot et al 2006).

This traditional stability analysis technique shows that the chatter instability depends on the structural damping in the system and the spindle speed. Chen and Tsao presented a dynamic model of cutting tool with (Chen Tsao 2006b) and without tailstock supported workpiece using beam theory (Chen Tsao 2006a). Here, the effects of workpiece parameters are studied on the dynamic stability of turning process by treating the workpiece as a continuous system. Carrino et al., (Carrino et al 2002) present a model that takes into account both the workpiece deflection and the cutting force between tool and workpiece. The three components of the cutting force are function of the cutting geometry.

The effect of the workpiece-tool-machine deflections is a shift of the workpiece cross-section and a moving back of the tool holder in the radial and the tangential direction (2D model).

In these processes, the cutting forces measurement has important and tremendous applications within industry and research alike.

The cutting forces estimation allows supervising tool wear evolution (Toh 2004), establishes material machinabilities, optimizes cutting parameters, and predicts machined workpiece surface quality and study phenomena such as chip formation or vibrations appearance.

Sekar and Yang propose a compliant two degree of freedom dynamic cutting force model by considering the relative motion of workpiece with cutting tool. Tool and workpiece are modelled as two separate single degree of freedom spring-mass-damper systems (Sekar et al 2008).

In the literature, there are many studies concerning the cutting force measurement. Many dynamometers for this purpose have been developed (Buyuksagis 1998, Castro et al 2006, Couétard 2000a, Korkut 1996).

In the measurement of the cutting forces (Seker et al 2004), only elastic deflections of the cutting tool due to the cutting forces were measured by means of the load cells located at suitable position on the cutting tool.

However the dynamometer can measure three perpendicular cutting force components and three torque components simultaneously during turning, and the measured numerical values can be stored in computer by data acquisition system (Couétard-00a). This dynamometer was designed to measure up to 5,000 N maximum force and 350 N·m torque. The system sensitivity is ±4% in force and ±8% in torque.

During the cutting process, the cutting tool penetrates into the workpiece due to the relative motion between tool and workpiece and the cutting forces and torques are measured on a measuring plane in the Cartesian coordinate system.

The cutting forces have been measured by the dynamometers designed for different working principles as strain gauge based (Couétard 2000a).

Thus it is necessary to have a good methodology to measure the workpiece-tool-machine rigidity before measuring forces and torques. This new methodolgy is precisely the purpose of these following sections.

The torsor concept is the basic tool of our approach of the matter removal. Also, before entering the sharp one of the subject, a short reminder of the torsor concept is given in chapter 3.

In chapter 4 the experimental device is presented. After (see section 4.2) we conceive the workpiece. The workpiece geometry and dimensions retained for these test-tubes were selected using the finite element method coupled to an optimization method, by SAMCEF® software.

In the following section 4.3 a methodology based on the virtual work (three translations and three rotations) is exhibited to study the static aims and to characterize the static equivalent stiffness values in order to identify the three-dimensional elastic behaviour of the machining system. The applied efforts are quantified with a force sensor.

The torsor of small displacements, three linears and three rotations displacement, is measured by six displacement transducer. A stiffness global matrix is deduced with its various results. The sum of the two stiffness matrix displacements block tool and block workpiece determines the stiffness matrix of machining system displacement. By the Castigliano's theorem we determine the angle that characterizes the principal direction of deformation.

In section 4.4 the stiffness centre is obtained using the least squares method in the coordinate system based on the tool in O point that is the origin of the coordinate system.

The knowledge of the machining system elastic behaviour is essential to understand the cutting process. The analysis of the machines equipments and dynamic behaviour it is an important method to redesign the product or the manufacturing process and to assure the proper quality, maintenance and service. When machines or only parts of them are studied, the dynamic behaviour is analysed in chapter 5.

Chapter 6 is dedicated to the experimental displacements analysis of the block tool/block workpiece with self-excited vibrations. In connection with the turning process, the self-excited vibrations domain is obtained starting from spectra of two accelerometers. One three axes accelerometer is placed on the tool and one unidirectional accelerometer is placed on the front of bearing of spindle. The existence of a displacements plane attached to the tool edge point is revealed.

This plane proves to be inclined compared to the machines tool axes. This plane contains an ellipse that is the place of the points of the tool tip displacements. We establish that the tool tip point describes an ellipse. This ellipse is very small and can be considered as a small straight line segment for the stable cutting process (without vibrations). In unstable mode (with vibrations) the ellipse of displacements is really more visible.

A difference in phase occurs between the tool tip displacements on the radial direction and on the cutting one.

The feed motion direction and the cutting one are almost in phase. The values of the long and small ellipse axes (and their ratio) shows that these sizes are increasing with the feed rate value. A weak growth (6%) of the long and small axes ratio is obtained when the feed rate value decreases. The axis that goes through the stiffness centre and the tool tip represents the maximum stiffness direction.

The maximum (resp. minimum) stiffness axis of the tool is perpendicular to the large (resp. small) ellipse displacements axis. The self-excited vibrations appearance is strongly influenced by the system stiffness values, their ration and their direction.

FFT analysis of the accelerometers signals allows reaching several important parameters and establishing coherent correlations between tool tip displacements and the static - elastic characteristics of the machine tool components tested.

A testing device in turning, including a six-component dynamometer, is used to measure the complete torsor of the cutting actions in the case of self-excited vibrations in section 7.

Many results are obtained regarding the mechanical actions torsor. A confrontation of the moment components at the tool tip and at the central axis is carried out. It clearly appears that analysing moments at the central axis avoids the disturbances induced by the transport of the moment of the mechanical actions resultant at the tool tip point.

For instance, the order relation between the components of the forces is unique. Furthermore, the order relation between the moments components expressed at the tool tip point is also unique and the same one. But at the central axis, two different order relations regarding moments are conceivable.

A modification in the rolling moment localization in the (**y, z**) tool plan is associated to these two order relations. Thus, the moment's components at the central axis are particularly sensitive at the disturbances of machining, here the self-excited vibrations.

3 VECTOR ANALYSIS

ALAIN GERARD

Because the emphasis is on applications and because space is limited, we shall state most of fundamental theorems without proof. The references should be consulted to complement this initiation (Perez 1989, Brousse 1973).

3.1 Recall vector space

One calls affine space f a set of elements called point such as with any ordered pair (AB) of two points A and B (bi-point) one makes correspond a vector **AB** of a vector space E.

3.1.1 *Euclidian vector space*

A vector space E is known as Euclidean if it is provided with a scalar product f which, with two vectors **u** and **v** of E makes correspond the real number f(u, v) such as:

$$\begin{aligned} f(\mathbf{u}, \mathbf{v}) &= f(\mathbf{v}, \mathbf{u}), \\ f(\mathbf{u}, \lambda\mathbf{v}) &= \lambda f(\mathbf{u}, \mathbf{v}) \\ f(\mathbf{u}, \mathbf{v} + \mathbf{w}) &= f(\mathbf{u}, \mathbf{v}) + f(\mathbf{u}, \mathbf{w}) \end{aligned} \qquad (1)$$

3.1.2 *Affine space*

One calls affine space $\tilde{E}$ a set of elements called point such as with any ordered pair (AB) of two points A and B (bi-point), one can make correspond a AB of a vector space E; A, B, C indicating three points of $\tilde{E}$ one must have:

- **AB** = – **BA**,
- **AC** = **AB** + **BC**,
- O being an unspecified point of $\tilde{E}$ there exists a point A and only one of $\tilde{E}$ defined by **OA** = **v** for any vector v pertaining to E.

3.1.3 *Reference mark of an affine space*

The unit formed by a point O of $\tilde{E}$ and of a basis of E constitutes a reference mark of $\tilde{E}$.

The point O is taken as origin of the reference mark. The reference mark of affine space associated with physical space is written R = (O, $\mathbf{e_x}$, $\mathbf{e_y}$, $\mathbf{e_z}$) or more briefly R = (O, **xyz**).

Three vectors **u, v, w** form with the O point a direct reference mark if an observer placed on **OA** = **u** the feet placed out of O and looking towards **OB** = **v** sees **OC** = **w** on its left. If **OC** is on its line the reference mark is opposite. This rule is called "rule of Ampère's people" or "rule of the corkscrew" (and sometimes the "right hand screw rule").

3.1.4 *Pointers*

One calls pointer the couple of a vector **V** of E and of a point A of $\tilde{E}$ associate with E noted (A, **V**). As example the force F which exerts a material system on a material point A can be represented by the pointer (A, **F**).

3.1.5 *Scalars field - vectors field*

One calls scalars field the application which makes correspond to any point A of $\tilde{E}$ a scalar θ.

Example: the temperature in any point A of space.

3.1.6 *Scalar or dot product*

One notes simply **u.v** the scalar (or dot) product of the two vectors **u** and **v**. Symbolically **u.v** = |u|·|v|·cos θ. Quantity f(**u, u**) is called square norm of the vector **u**. It is noted |u|. The positive square root of f(**u**, **u**) is called the length of the vector and denoted by |u| = $\sqrt{f(u,u)}$. A vector whose length is unity is called a normalized vector or unit vector. One physical interpretation of this scalar product is the calculation giving the work done by a force **u** during a displacement **v** by its point of application A.

3.1.7 *Vector or cross product*

Referring to the above situation where θ is the angle between the two vectors u and v, then the vector (or cross) product of **u** and **v** is defined by:

$$\mathbf{u} \wedge \mathbf{v} = |\mathbf{u}|\cdot|\mathbf{v}| \sin\theta\cdot\mathbf{n} \qquad (2)$$

where the symbol ∧ is used to denote a vector (or cross) product of the two vectors **u** and **v. n** is a unit vector along the normal to the plane containing **u** and **v** and its positive direction is determined as follows.

The right hand screw rule is applied to the sense of rotation from u to v in measuring the angle θ, thus defining the positive direction **n**. This rule indicates that **n** acts into the plane of the paper. This definition is unique.

However, the vector $\mathbf{v} \wedge \mathbf{u}$ has the same magnitude as $\mathbf{u} \wedge \mathbf{v}$ but the direction of n is reversed due to describing by moving to θ. Hence, $\mathbf{u} \wedge \mathbf{v} = -\mathbf{v} \wedge \mathbf{u}$ and the order of the terms in the product is important.

3.1.8 *Moment at a point*

By definition the moment at a point O (noted **Mo**) of the pointer (A, **V**) is the vector:

$$\mathbf{Mo} = \mathbf{OA} \wedge \mathbf{V}. \tag{3}$$

For example, the moment of a force **V** is defined by a vector product in the following manner.

If there is a force **V** acting at a point A with the position vector OA relative to an origin O, then the moment of **V** about O is defined by Eq. (3).

It is shown easily that moment at a point O' (**Mo'**) and the moment at a point O (**Mo**) are linked by the relation:

$$\mathbf{Mo} = \mathbf{Mo'} + \mathbf{OO'} \wedge \mathbf{V} \tag{4}$$

By definition, O being a point of an axis Δ of unit vector u the moment of the pointer (A, **V**) compared to the axis Δ is the scalar:

$$\mathbf{M_\Delta} = \mathbf{u} \cdot \mathbf{Mo} = \mathbf{u} \cdot (\mathbf{OA} \wedge \mathbf{V}) \tag{5}$$

This concept is independent of the point chosen on the axis.

3.2 Torsor

3.2.1 *Antisymmetric field*

A field of vectors $\mathbf{M_A}$ is antisymmetric if there is a vector **R** such as, whatever two points A and B one has:

$$\mathbf{M_A} = \mathbf{M_B} + (\mathbf{AB} \wedge \mathbf{R}) \tag{6}$$

the vector **R** is called vector of the antisymmetric field. Taking into account the definition one sees that R and MA have different polar and axial characteristics.

3.2.2 *Definition of a torsor*

One calls torsor reduced to the point O noted $[A]_O$ the whole of an antisymmetric field $\mathbf{M_O}$ and of his vector **R**; $\mathbf{M_O}$ and **R** are respectively called moment and vector (or general resultant) of the torsor $[A]_O$ reduced to the point O.

This abstract element is generally noted:

$$[A]_O = \begin{Bmatrix} R \\ M_O \end{Bmatrix} \tag{7}$$

3.2.3 *Properties*

The following results are immediately verifiable:

- Two torsors $[A_1]_O$ et $[A_2]_O$ reduced in the same point O are equal if their antisymmetric field and their vector are equal ($\mathbf{R_1} = \mathbf{R_2}$ and $\mathbf{M_{1O}} = \mathbf{M_{2O}}$).

- The sum of two torsors reduced to the same point is a torsor (reduced to the same point) whose elements are respectively the sum of the antisymmetric fields and the sum of the vectors (i.e. with evident notation : $\mathbf{M_O} = \mathbf{M_{1O}} + \mathbf{M_{2O}}$ and $\mathbf{R} = \mathbf{R_1} + \mathbf{R_2}$).

- To multiply a torsor by a scalar (λ) consists to multiply by this scalar the antisymmetric field and the vector (with evident notation: $\mathbf{M_O} = \lambda\mathbf{M_{1O}}$ and $\mathbf{R} = \lambda\mathbf{R_1}$).

3.2.4 *Invariants*

The following results are established easily:

- Projections of the antisymmetric field reduced at point A and at point B on its vector are equal ($\mathbf{R}\cdot\mathbf{M_A} = \mathbf{R}\cdot\mathbf{M_B}$).

- $\mathbf{AB}\cdot\mathbf{M_A} = \mathbf{AB}\cdot\mathbf{M_B}$). This invariant property is known under the name of equiprojectivity.

- The scalar product (or comoment) of two torsors reduced to the same point is the scalar $P = (\mathbf{R_1}\cdot\mathbf{M_{A2}} + \mathbf{R_2}\cdot\mathbf{M_{A1}})$. If one of the torsors is the torsor speeds and the other the torsor of the forces this scalar P represents the mechanical power.

3.2.5 *Torsor associated with a set of pointers*

Let us consider a set of pointers (A_i, $\mathbf{V_i}$). In an arbitrary point O the resulting moment $\mathbf{M_O}$ by introducing another O' point, we have:

$$\mathbf{M_O} = \sum_i \mathbf{OA_i} \wedge \mathbf{V_i} = \sum_i (\mathbf{OO'} + \mathbf{O'A_i}) \wedge \mathbf{V_i}$$
$$\mathbf{M_O} = \mathbf{M_{O'}} + \mathbf{OO'} \wedge \sum_i \mathbf{V_i} \qquad (8)$$

Putting $\mathbf{R} = \sum_i \mathbf{V_i}$ it comes:

$$\mathbf{M_O} = \mathbf{M_{O'}} + \mathbf{OO'} \wedge \mathbf{R} \qquad (9)$$

Therefore, with a set of pointers, one can associate a torsor of vector $\mathbf{R} = \sum_i \mathbf{V_i}$ and of moment about point O, $\mathbf{MO} = \sum_i \mathbf{OA_i} \wedge \mathbf{R}$.

3.2.6 *Central axis*

The geometric locus of points in which the resulting moment is collinear with the vector R (resulting general) supposed non equal to zero is defined by:

$$\mathbf{OA} = \frac{R \wedge M_O}{\|R\|} + \lambda\, \mathbf{R} \qquad (10)$$

where O is the point where the torsor was moved and A is the current point describing the central axis. Thus, **OA** is the vector associated with the bi-point [O, A] (figure 1).

This line (figure 1-(a)) corresponds to geometric points where the mechanical action moment torsor is minimal. The central axis calculation consists in determining the points assembly (a line) where the torsor can be expressed according to a slide block (straight line direction) and the pure moment (or torque) (Brousse, 1973). This line do not belongs to O point.

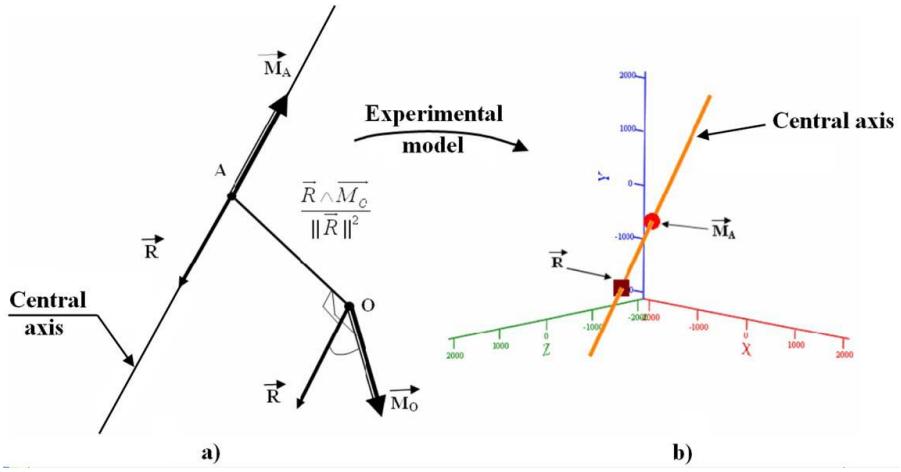

Figure 1 Central axis representation (a) and of the colinearity between vector sum R and minimum moment MA on central axis (b).

The distribution of the resulting moments in space admits the central axis like axis of revolution. It is easily to show that one can always possible reduce a torsor to two vectors of which one is located in a *P* plan while the other is perpendicular to the *P* plan.

Part 1 TURNING

4 STATIC CHARACTERIZATION

Olivier CAHUC, Jean-Yves K'NEVEZ, Raynald LAHEURTE, Alain GERARD

4.1 Introduction

Today, machines tool are very rigid there are less and less geometrically faulty. The vibratory problems are strongly related to the cutting. Ideally, cutting conditions are chosen such that material removal is performed in a stable manner. However, sometimes chatter is unavoidable because of the geometry of the cutting tool and workpiece.

In (Perez et al., 2007) the bulk of the motion during chatter comes from the workpiece since it has a static stiffness that is up to 3.2 times less than the cutting tool. Since it is highly impractical to instrument the workpiece during cutting the end goal is to develop an observer that can transform measurements made at the cutting tool into a prediction about the motion of the workpiece. Dassanayake et al., 2008 approaches in the 1D case the dynamic response of the tool holder to the request of the tool which follows a regenerative surface. They consider only tool motions and disregards workpiece vibration. Insperger continues in the 2D case keeping workpiece rigid but he takes into account the flexibility of the tool (Insperger et al., 2008).

For an operation of milling (Salgado et al., 2005), the deflections of the machine-tool, the toolholder and the toolholder clamping in the spindle, the tool clamping in the toolholder, and the tool itself, were measured experimentally under the effects of known forces. The results of this study show that the stiffness of both the machine and the clamping in the machine-spindle-toolholder-tool system have a similar importance in the displacement of the tool tip (subjected to a cutting force) to the deflection of the tool itself. Thus, it is necessary to identify the elastic behaviour of machine parts (Cano et al., 2008). These vibrations are generated and self induced by the cutting process. A conventional lathe with high rigidity is used to study these dynamic phenomena. The Workpiece-Tool-Machine (**WTM**) system is presented in the figure 2 for a turning operation.

The elastic structure of **WTM** system has several degrees of freedom and has many specific vibration modes. The vibrations of each element of the structure are characterized by its natural frequency depending on the Stiffness matrix [K], the Mass matrix [M] and the Damping matrix [C]. In a first time, only the stiffness matrix [K] is studied. The matrix [C] is studied further in the dynamic case (section 5.3.3).

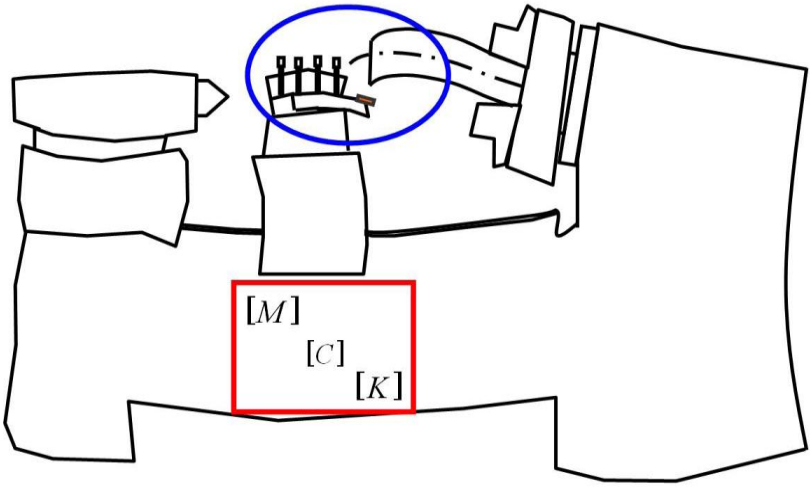

Figure 2 Workpiece-Tool-Machine considering dynamic cutting process.

Our experimental approach is based on the matrix development that is presented in (Pestel et al., 1963).

To identify the **WTM** system static behaviour, the machining system is divided into two blocks, the Block Tool (**BT**) and the Block Workpiece (**BW**) figure 3.

These two blocks are related to the turn bed supposed to be infinitely rigid.

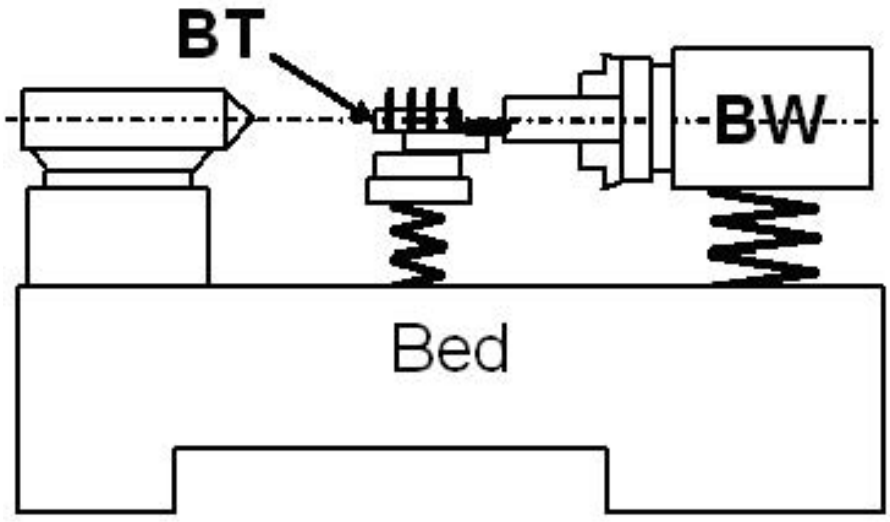

Figure 3 Presentation of the experimental device.

4.2 Components of the system WTM

4.2.1 Block workpiece: **BW**

As many workers (Benardos et al., 2006; Mehdi et al., 2002a; Yaldiz et al., 2006) a cylindrical geometry of the workpiece is chosen.

The **BW** represents the revolving part of the **WTM** system; it includes the holding fixture, the workpiece and the spindle (figure 4 a, b).

To make the whole frame rigid, a very rigid unit (workpiece, holding fixture) is conceived in front of the **WTM** elements (figure 5).

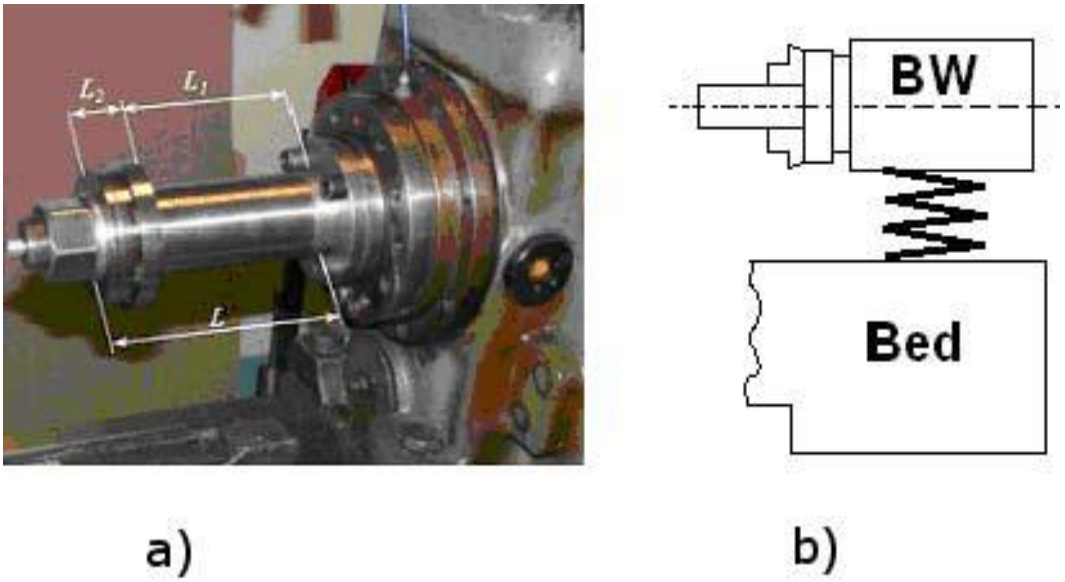

Figure 4 **BW** representation.

The workpiece geometry and his holding fixture are selected with D_1 = 60 mm, D_2 = 120 mm and L_2 = 30 mm (cf. figure 5).

The dimensions of these test tubes were selected using a finite element analysis coupled to an optimization, with SAMCEF® software in order to confer on the unit a maximum rigidity.

It is necessary to determine the holding fixture length L_1 to obtain a significant stiffness in flexion.

The objective is to move away the first **BW** vibration mode of the lathe fundamental natural vibration mode (see Bisu, 2007).

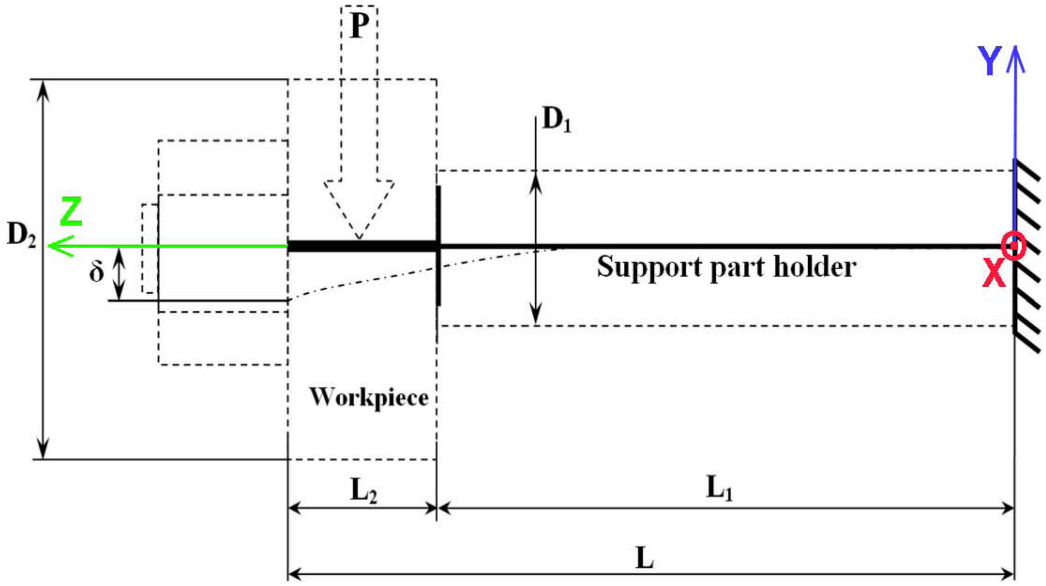

Figure 5 Geometry of holding fixture/workpiece.

As (Salgado et al., 2005) and others the stiffness is calculated on the basis of the displacement δ for a given force P:

$$\delta = \frac{P \times L^3}{3E \times I} \tag{11}$$

with inertial moment :

$$I = \frac{\pi \times D_1^4}{64} \tag{12}$$

The figure 6 represents the displacements and stiffness values relating to the length of holding fixture/workpiece, for a load P = 1,000 N, for material having a Young modulus E = 21×10^5 N/mm^2 and a holding fixture diameter D_1 = 60 mm.

A holding fixture length: L_1 = 180 mm, for a stiffness in flexion of 7×10^7 N/m, is reminded.

This value is including in the higher part of the interval of the acceptable rigidity values for a conventional lathe (cf. figure 7), (Ispas et al., 1999; Koenigs et al., 1971; Konig et al., 1997).

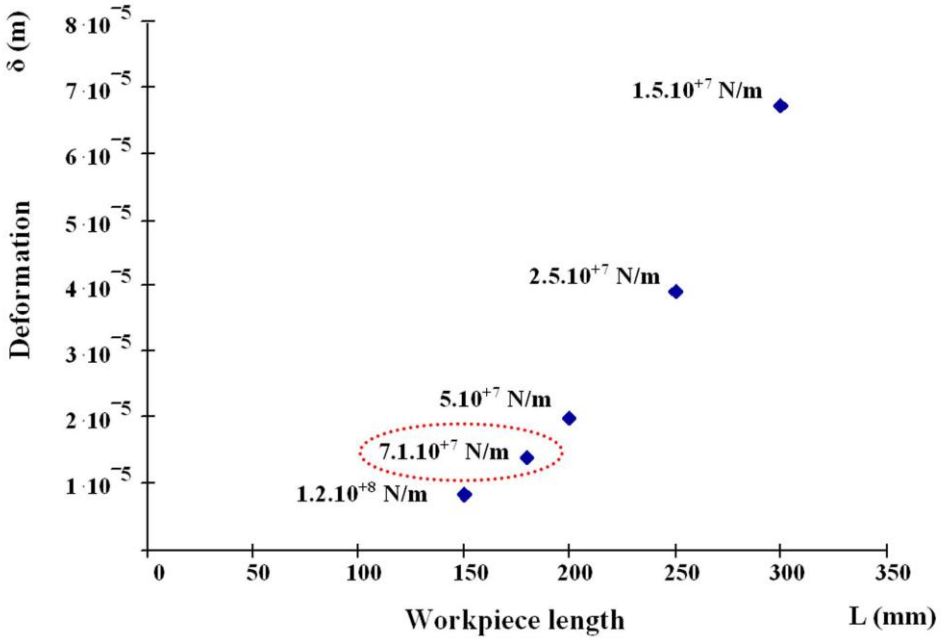

Figure 6 Displacements according to the holding fixture length.

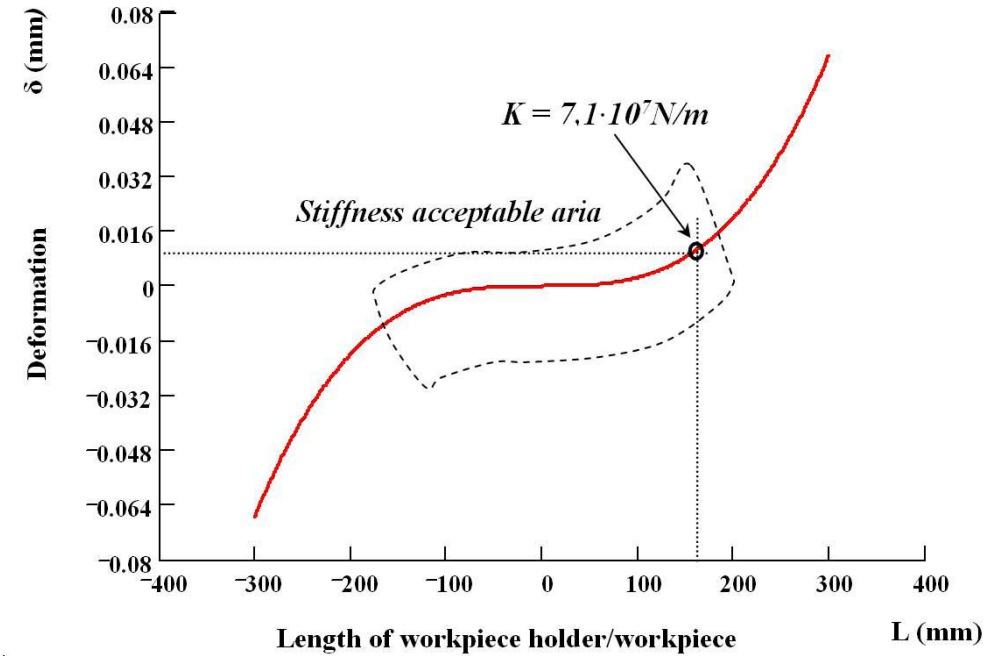

Figure 7 Acceptable aria representation of the workpiece deformation.

4.2.2 *Block Tool:* ***BT***

In this case, the **BT** part includes the tool, the tool-holder, the dynamometer, the fixing plate on the cross slide (figure 8 a). The six-component dynamometer (Couétard, 2000a) is fixed between the cross slide and the tool-holder. This is necessary thereafter to measure the cutting mechanical actions. The stiffness of **BT** is evaluated into the next subsection.

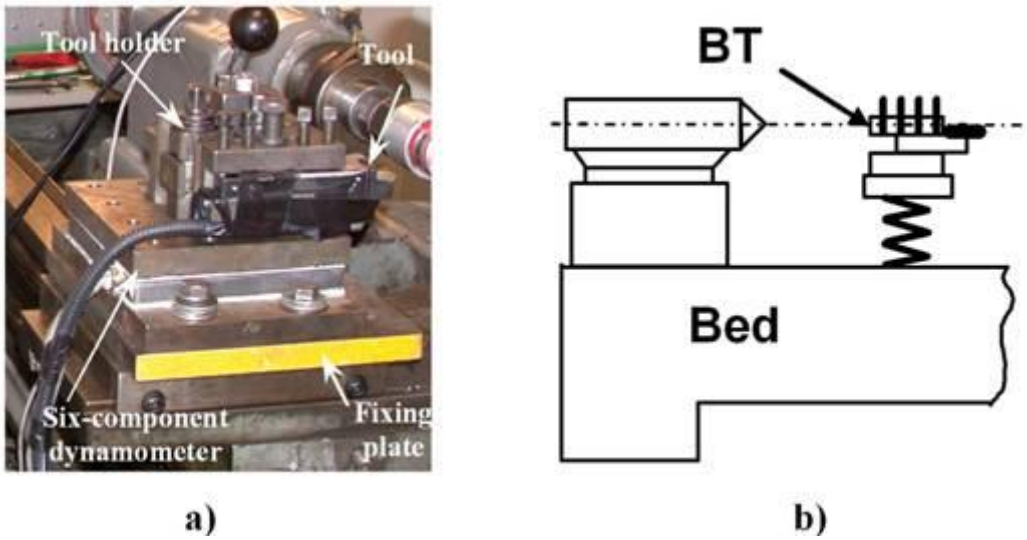

Figure 8 Block Tool BT representation.

4.3 Static characterization of machining system

The static study aims at characterizing the static equivalent stiffness values in order to identify the three dimensional elastic behaviour of the machining system. Generally, the static tests consist in charging by known efforts the two blocks and measuring only the associated displacements components (Gorodetskii et al., 2008; Yaldiz et al., 2006b). Here the static tests consist in loading by known efforts the two blocks but measuring the small displacements torsor (i.e. three linear displacements, and three rotations). The applied efforts are quantified with a force sensor. The small displacements torsor is measured by six displacement transducers. A stiffness global matrix is deduced with its various results. It is a real 3D pattern. For instance, Carrino et al., present a model that takes into account both the workpiece deflection and the cutting force between tool and workpiece. The three components of the cutting force are a depend on the cutting geometry. The effect of the workpiece-tool-machine deflections is a shift of the workpiece cross-section and a moving back of the tool holder in the radial and the tangential direction (2D model) (Carrino et al, 2002).

4.3.1 *Stiffness matrix*

The experimental approach is based on the matrix development presented in (Robinson, 1971). The deformation of a structure element is represented by displacements of nodes determining this element. The "associated forces" correspond to displacements which act as these nodes.

The transformation matrix which connects generalized displacements of an element to the "associated forces" is the rigidity matrix or the stiffness matrix of the element.

In the same way the matrix which connects generalized displacements of the structure to the applied generalized discrete forces is the stiffness matrix of the structure simply named as "stiffness matrix": [K].

The relation between forces and displacements is given by (Pestel et al., 1963):

$$\{T\} = [K] \times \{D\}, \tag{13}$$

where {T} represents the mechanical action torsor, [K] the stiffness matrix and {D} the small displacements torsor.

The general form of the square (6 × 6) stiffness matrix [K] is:

$$[K]_{A,xyz} = \begin{bmatrix} K_{FC} & K_F \\ K_C & K_{CF} \end{bmatrix}_{A,xyz}, \tag{14}$$

where $[K_F]$, $[K_C]$, $[K_{CF}]$ and $[K_{FC}]$ are respectively square (3 x 3) displacement matrix, rotation and rotation/displacement and displacement/rotation expressed at the point A in x, y, z machine axes.

4.3.2 *Experimental determination of the stiffness matrix*

Methodology The matrix elements of the small displacement torsor are identified thanks to the experimental device presented in the figure 9.

The considered system is a cube. Displacements are measured by six displacement transducers. Two displacement transducers are positioned symmetrically on each of the three directions.

The force is applied to each **x, y, z** direction in two different levels by a screw-swivel system controlled by a force sensor. Each loading point coordinates are known starting from the cube centre O_c.

This allows for each applied force to determine the moment and thus the complete torsor of mechanical actions {T}.

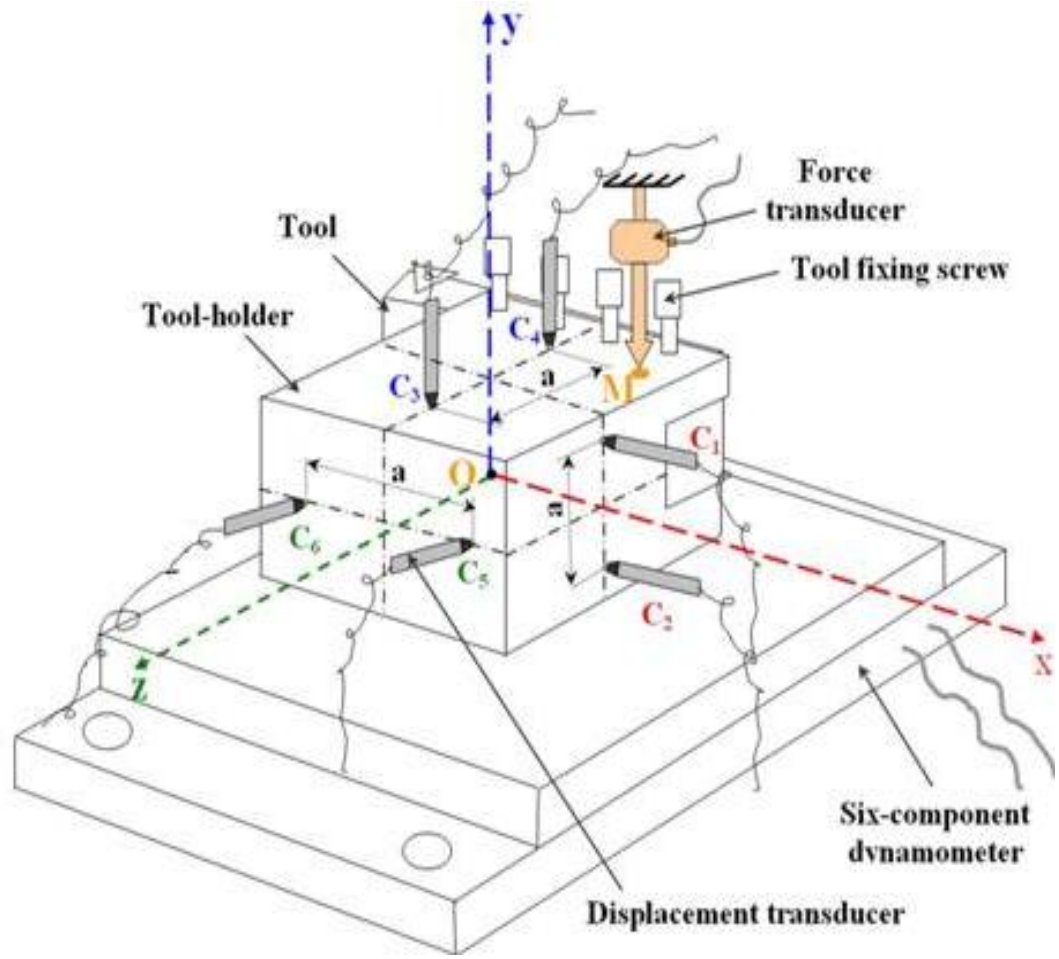

Figure 9 Experimental device for the static characterization.

Induced displacements are solid body displacements and it is noted that rotations are low ($> 10^{-5}$ rad) but exist.

The existence of these rotations is important and in agreement with the torque via the virtual work theory.

The measure principle is presented in the figure 10 and is used to determine the components of the small displacements torsor {D} which is composed by the three rotations ρ_x, ρ_y, ρ_z and the three displacements ε_x, ε_y, ε_z.

Thus, the displacements m and rotations θ are determined, for each loading direction, by using the relations:

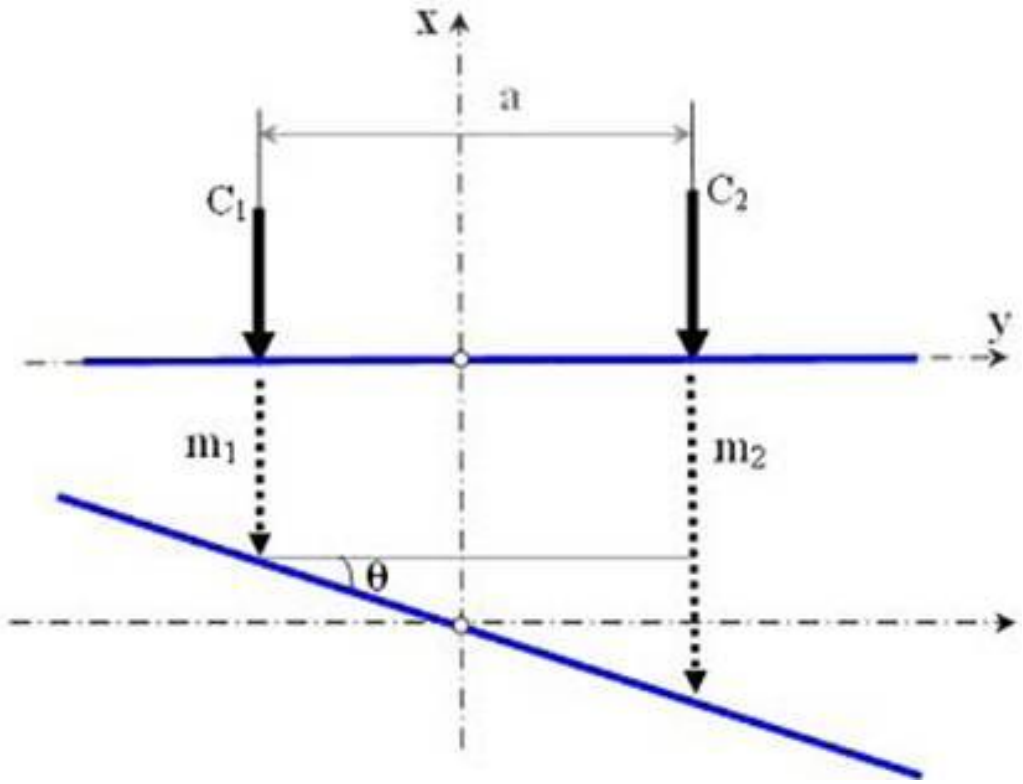

Figure 10 Position of displacement transducer.

$$m = \frac{m_1 + m_2}{2}, \tan(\theta) \approx \theta = \frac{m_2 - m_1}{a} \tag{15}$$

From these relations and considering the six measurements points it results:

$$\begin{bmatrix} \rho_x \\ \rho_y \\ \rho_z \\ \varepsilon_x \\ \varepsilon_y \\ \varepsilon_z \end{bmatrix} = \begin{bmatrix} 0 & 0 & \frac{-1}{a} & \frac{1}{a} & 0 & 0 \\ 0 & 0 & 0 & 0 & \frac{-1}{a} & \frac{1}{a} \\ \frac{-1}{a} & \frac{1}{a} & 0 & 0 & 0 & 0 \\ \frac{1}{2} & \frac{1}{2} & 0 & 0 & 0 & 0 \\ 0 & 0 & \frac{1}{2} & \frac{1}{2} & 0 & 0 \\ 0 & 0 & 0 & 0 & \frac{1}{2} & \frac{1}{2} \end{bmatrix} \bullet \begin{bmatrix} m_1 \\ m_2 \\ m_3 \\ m_4 \\ m_5 \\ m_6 \end{bmatrix} \tag{16}$$

The tests are carried out with specific assemblies which are designed for each direction of measurement. The loading (respectively unloading) is carried out by step of 30 daN (resp. – 30 daN) until (resp. from) level of 200 daN, and this procedure is used for each test following known directions. To check the repeatability and accuracy of identifications all tests and measurements are carried out five times and the average is selected for each point at figure 11.

To exploit measurements as well as possible, the displacements curves are plotted depending on the applied force for each loading direction. A line of least squares is adjusted to determine the displacements components values for a given force. Thus, six torsors of small displacements are identified for six loadings cases. The linear behaviour observed in loading is different from the linear behaviour noted in unloading. This different linearity between loading and unloading is due to the existence of deviations and friction forces in each point surfaces of the assembly. These deviations due to the installation of the parts of the associated assembly and friction force are different in charge and discharge.

When this difference in linear behaviour appears (hysteresis), we use the line (figure 11) which passes by the middle (*C* point) of segment *AB* (charge-discharge). *OC* is the line which the slope, by assumption, corresponds to the "real" stiffness. Segment *AB* represents the double of the friction forces and deviations for the deformation δ, (Kudinov, 1970).

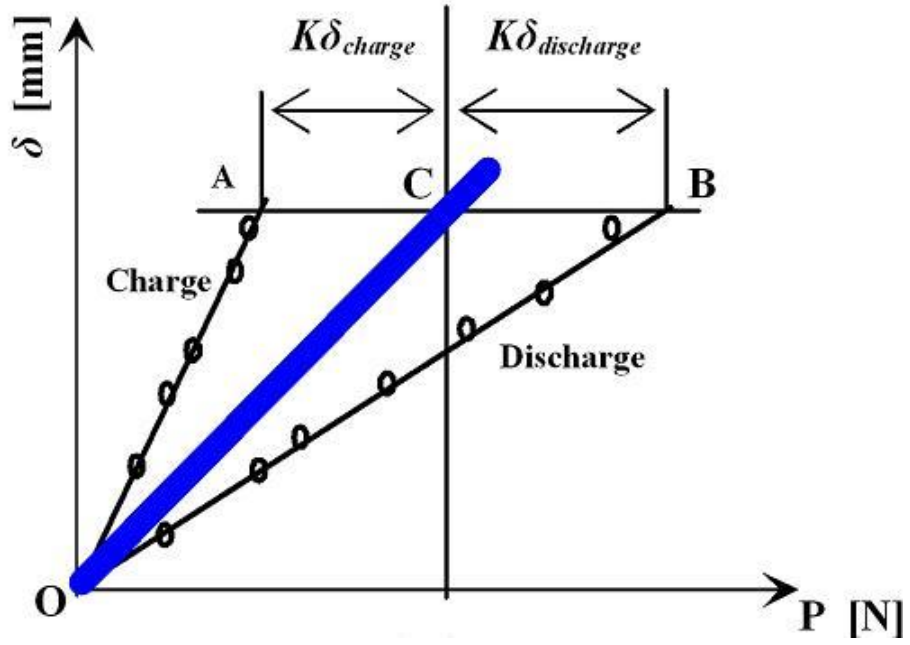

Figure 11 Diagrammatic representation of linear behaviour in charge and discharge.